Combining Eulerian and Lagrangian numerical approaches to investigate the influence of hydrodynamic variability on the transport of sediment and fish eggs

E. W. North, R. R. Hood, S.-Y. Chao, L. P. Sanford
University of Maryland Center for Environmental Science, Horn Point Laboratory
P. O. Box 775, Cambridge, MD, 21613, USA [tel: +1 410 228 8200, fax +1 410 221 8490, e-mail: enorth@hpl.umces.edu, raleigh@hpl.umces.edu, chao@hpl.umces.edu, lsanford@hpl.umces.edu]

ABSTRACT

Numerical approaches were developed for the purpose of investigating the influence of hydrodynamic variability on the transport of fish eggs and sediment near a frontal zone. The Princeton Ocean Model (POM) was adapted to a straight-channel estuary and enhanced with sediment settling, erosion, deposition and burial components. In addition to Eulerian sediment modeling, a Lagrangian particle tracking model was constructed within the numerical circulation model to simulate the transport of individual sediment particles and fish eggs in the flow field. A random displacement model (RDM) was implemented within the particle tracking model to parameterize sub-grid scale turbulence. Tests of the Well Mixed Condition suggest that the RDM significantly reduced numerical artifacts that can occur when simulating particle motion in regions with high gradients in turbulence. In addition, comparison between Lagrangian particle distributions and Eulerian tracer concentrations suggest that Lagrangian particle motion reasonably approximated tracer dispersal, especially in the vertical direction. The coupled Eulerian-Lagrangian model has the potential to be a powerful tool for investigating the influence of hydrodynamic variability on the transport and potential survival of fish early-life stages in frontal zones.

INTRODUCTION

Advancing understanding of biological-physical interactions in frontal zones is an important avenue of research. Frontal regions are ubiquitous throughout the world's estuaries and coastal oceans where important recreational and commercial fisheries occur. Fronts structure physical conditions such as temperature, salinity, and nutrient concentrations (Largier 1993) as well as the distribution of planktonic organisms including phytoplankton (Hood et al. 1991, Uye et al. 1992, Franks and Walstad 1997), crustacean zooplankton (Jillett and Zeldis 1985, Epifanio 1987, Mackas and Louttit 1988, Okazaki et al. 1998, Shanks et al. 2000, Epstein and Beardsley 2001), and fish larvae (Govoni et al. 1989, Govoni and Grimes 1992, Govoni 1993, 1997, Kingsford and Suthers 1996, Munk et al. 1999, Nakata et al. 2000, Lough and Manning 2001, Bjorkstedt at al 2002, Munk et al. 2002, North and Houde *in press*). The physical and biological characteristics of frontal regions are hypothesized to be important areas for growth of plankton due to enhanced nutrient concentrations and convergent circulation that can promote production, increase aggregation of organisms, and intensify trophic interactions (Wolanski and Hamner 1988, Boynton et al. 1997, Winkler et al. 2003).

Lagrangian particle tracking models coupled with hydrodynamic models have been used to gain new insight on how planktonic dispersal and growth are mediated by physical conditions (Werner et al. 1996, Hannah et al. 1998, Heath and Gallego 1998, Hare et al. 1999, Bartsch and Coombs 2001, Hinckley et al. 2001, Werner et al. 2001). These models move individual particles through time and space using current velocities output from the hydrodynamic model. To accurately portray particle motion, Lagrangian particle tracking models include a sub-grid scale turbulence model to simulate turbulent motion at scales smaller than those resolved by the hydrodynamic model.

Correct parameterization of sub-grid scale turbulence in Lagrangian particle tracking models presents challenges in frontal regions due to numerical artifacts. When implemented in hydrodynamic models that contain sharp gradients in turbulence (e.g., fronts), sub-grid scale turbulence models that employ a

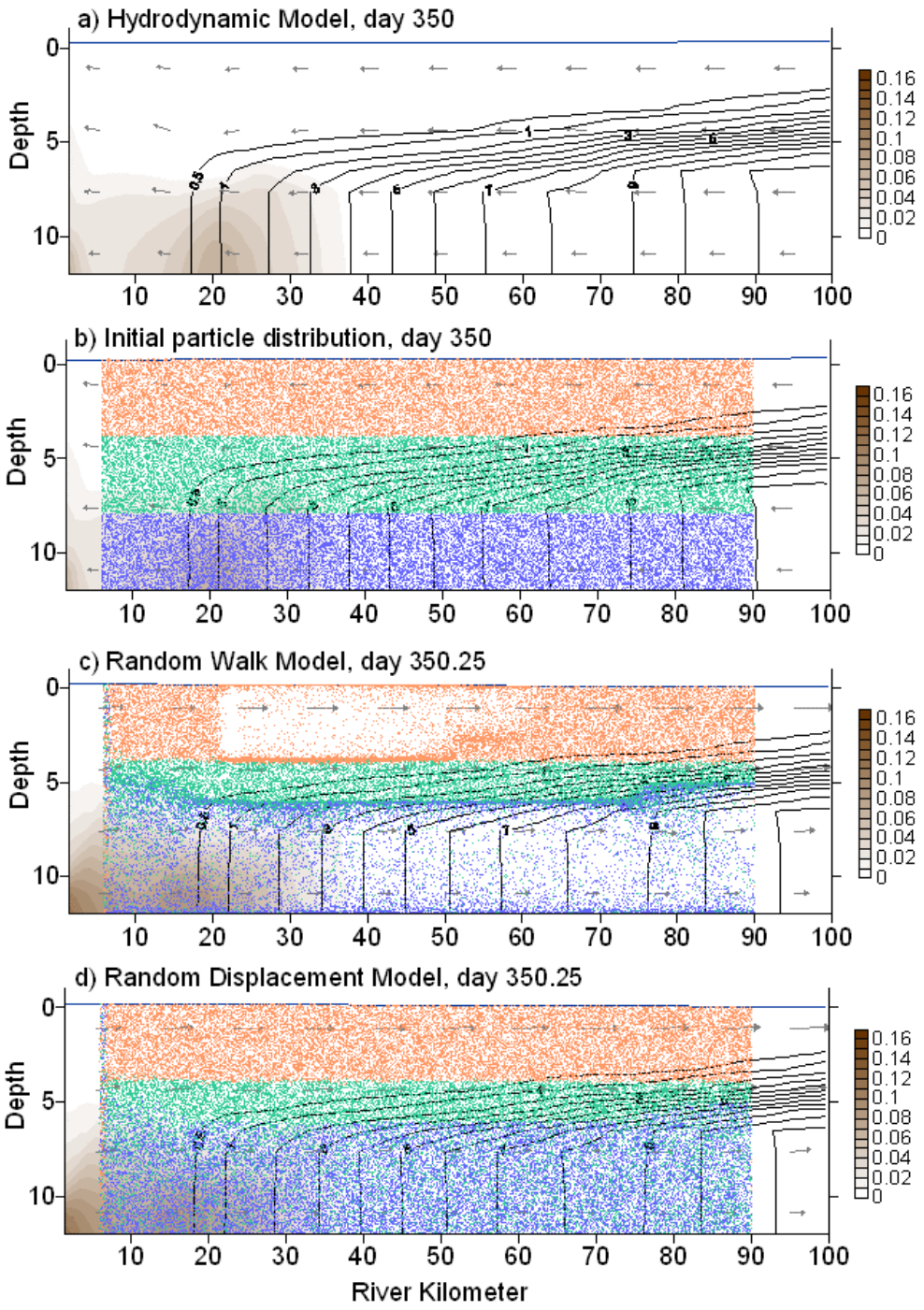

Figure 1. ETM hydrodynamic model output and particle distributions. a) Hydrodynamic model output at day 350. Line contours are salinity, arrows are vectors, and shaded contours are suspended sediment concentrations (kg m^{-3}) with color scale on right. b) Initial random distribution of 50,000 particles in the particle tracking model domain. c) Particle distribution after 6 hr when a random walk model was used to simulate sub-grid scale turbulence in the vertical direction. d) Particle distribution after 6 hr when a random displacement model (Visser 1997) was used to simulate sub-grid scale turbulence in the vertical direction. Particle colors correspond to depth of initial release.

random walk model result in artificial aggregation of neutrally buoyant particles in areas of low diffusivity, violating the Well Mixed Condition (Visser 1997, Brickman and Smith 2001). Particle tracking models that adhere to the Well Mixed Condition maintain "an initially uniform concentration of [neutrally buoyant] particles uniform for all time" (Brickman and Smith 2002). Failure of the random walk model to meet the Well Mixed Condition is clearly evident in a model of the salt front (landward margin of salinity intrusion) at the head of many coastal plain estuaries (Fig. 1c). In contrast, a random displacement model (RDM) used to simulate sub-grid scale turbulence (Visser 1997) is much more successful (Figure 1d).

The salt front at the head of estuaries is an ideal test case to advance numerical approaches and enhance our understanding of biological-physical interactions in frontal regions. Strong gradients in vertical diffusivity (turbulence) in this region present a numerical challenge for particle tracking models. But, improved modeling in this region likely will advance our understanding of fisheries recruitment. This region is an important anadromous fish nursery area, and field evidence suggests that physical conditions may have a strong influence on larval fish survival and juvenile recruitment (North and Houde 2001, *in press*). Circulation patterns near the salt front can create an estuarine turbidity maximum (ETM). ETMs, characterized by elevated turbidity and suspended sediment concentrations compared to those up- and down-estuary, are found in coastal plain estuaries throughout the world (Schubel 1968), including estuaries in Canada, France, Germany, UK, and USA (Schubel 1968, Allen et al. 1980, D'Anglejan 1981, Uncles and Stephens 1993, Jay and Musiak 1994, Burau et al. 1998, Geyer et al. 2001, Kappenberg and Grabemann 2001, Lin and Kuo 2001, Sanford et al. 2001, Kostaschuk 2002). The ETM region is an important nursery area for larval fish in the St. Lawrence River estuary (Dodson et al. 1989, Dauvin and Dodson 1990, Sirois and Dodson 2000), the San Francisco Bay/Delta (Jassby et al. 1995, Bennett et al. 2002), and upper Chesapeake Bay (Boynton et al. 1997; North and Houde 2001, *in press*). The numerical hydrodynamic model employed in this research reproduces an ETM (Fig. 1a), and the Lagrangian particle tracking model simulates the movement of fish eggs in this region.

This paper describes a method for implementing a random displacement model in a Lagrangian particle tracking model, summarizes tests of the Well Mixed Condition (WMC), and presents results of comparisons between Eulerian tracer and Lagrangian particle distributions. Examples of how the coupled Eulerian-Lagrangian particle tracking models can be used to better understand the influence of hydrodynamic variability on the transport of fish eggs in a frontal zone will be presented at the 2003 ICES Annual Science Conference.

METHODS

Hydrodynamic and sediment transport model. The three-dimensional hydrodynamic ETM model is based on the code of the Princeton Ocean Model (POM) (Blumberg and Mellor 1987, Mellor 1998) under hydrostatic and Boussinesq approximations. Eddy viscosity and diffusivity is determined by the level-2.5 turbulent closure scheme of Mellor and Yamada (1974). Our enhancements to POM include building suspended sediment and sediment transport components that track bottom sediment concentrations, adding constant loading of suspended sediment at the up-stream boundary, parameterizing bottom sediment burial with a Newtonian dampening term, and constructing a more reasonable formulation for background diffusivity.

The ETM model domain (Figure 3) contains a 98-km long and 4.8-km wide channel with a

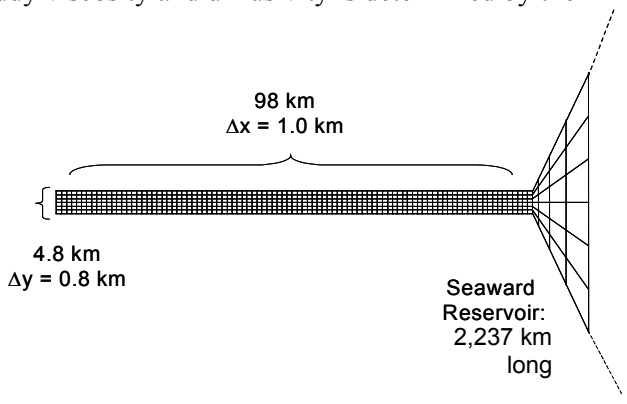

Fig. 3. Schematic of hydrodynamic model

gradually widening seaward reservoir that is 2,237 km long and has a maximum width of 66 km. The entire basin is 12 m deep and contains 145 grid spacings in the x-direction (seaward) and 6 in the y-direction (across channel). Vertical resolution is provided by 12 sigma-coordinate layers. In the first 98 km of the channel, the longitudinal resolution (Δx) is 1 km and the lateral resolution (Δy) is 0.8 km. In the seaward reservoir, Δx and Δy gradually increase at a rate of 12 and 5.5 percent per grid, respectively. The seaward reservoir, although of minor importance to the circulation and sediment transport within the channel, serves as a buffer zone to enhance the long-term computational stability of the model. The temporal resolution of the model is split. Vertically averaged currents and sea level are resolved with a time step of 5 s, and salinity, sediment concentration, and vertically explicit current velocities are resolved with a time step of 40 s.

A barotropic tidal generation force is included in the longitudinal momentum equation to produce semidiurnal tidal currents in the channel. Tidal current speed and upstream dissipation are parameterized so that sea level height and tidal current velocities in the model are similar to those of predicted tides in upper Chesapeake Bay. Lateral walls bounding the channel are impenetrable, impermeable and free-slip. Further information regarding model parameterization and boundary condition is forthcoming (North et al. *in press*) and can be obtained by contacting the authors.

Initially, the model channel was filled with motionless clear water of 12 practical salinity units (psu). The model was run with river inflow = 0.07 m s^{-1} and constant sediment loading until the model reached a quasi steady-state at day 350. In this quasi steady-state, sediment input equaled sediment burial and the location of the salt front was stable: it oscillated with the tidal current in a repetitive cycle but did not progress up or down estuary. All model scenarios use the quasi steady-state solution at day 350 as the initial condition.

Particle tracking model formulation. The Lagrangian particle tracking model is a subroutine of the hydrodynamic model that is called every internal time step (40 s). Current velocity, sea surface height, horizontal and vertical diffusivity, kinematic viscosity and water density derived in the hydrodynamic model are passed to the particle tracking model. Changes in particle locations due to advection are calculated every 10 s using an 8-point interpolation of U, V, and W velocities at the particle location. Near the bottom, the law-of-the-wall is applied so that u-, v-, and w-velocities decrease logarithmically to the depth of the roughness height (0.001 m).

The hydrodynamic model is tuned to examine along-channel processes. Because cross-channel displacement of particles is < 38 m in 10 days, sub-grid scale turbulence in the Lagrangian model is parameterized in the vertical (z) and along-channel (x) directions, not in the cross-channel direction (y).

Turbulence in the along-channel direction. A random walk model (RWM) (Visser 1997) was implemented within the particle tracking model to simulate sub-grid scale turbulence in the horizontal direction (x):

$$x_{n+1} = x_n + c\, R\{ 2r^{-1} K_h\, \partial t \}^{1/2}$$

where z = particle position at horizontal location n, K_h = horizontal diffusivity at the particle location, ∂t = time step of RWM (∂t = 1 sec), c = scaling coefficient (c = 0.2), and R is a random process with mean = 0 and standard deviation r = 1. The scaling coefficient of c = 0.2 results in greater horizontal spreading of particles than in model runs without horizontal sub-grid scale turbulence. For example, when particles were release throughout the water column at river kilometer 16, the maximum distance between particles after 1 hr was 0.71 km when horizontal turbulence was included in the model as opposed to a maximum distance of 0.46 km due to advection alone. A random walk model was used to represent sub-grid scale turbulence in the horizontal direction because we used constant horizontal diffusivity in the ETM model. In situations with constant diffusivity, random walk and random displacement models are equivalent (Visser 1997).

Turbulence in the vertical direction. A random displacement model (Visser 1997) was implemented within the particle tracking model to simulate sub-grid scale turbulence in the vertical (z) direction:

$$z_{n+1} = z_n + K_v'(z_n)\,\partial t + R\{\, 2r^{-1}\, K_v[\, z_n + 0.5\, K_v'(z_n)\,\partial t\,]\;\partial t\,\}^{1/2}$$

where z = particle depth at vertical location n, K_v = vertical diffusivity, ∂t = time step of the RDM, K_v' = $\partial K/\partial z$, and R is a random process with mean = 0 and standard deviation r = 1. To satisfy the RDM criterion $\partial t << \min(1/K_v'')$ (Visser 1997), the time step of the RDM (∂t) was set at 1 s after examination of a 10-d time series of $1/K_v''$ that included wind events.

The RDM was found to be most sensitive to parameterization of the second term, the gradient in vertical diffusivity at the particle location (K_v'). Many methods were used to estimate the rate of change of vertical diffusivity at the particle location, including 8-point linear interpolation, smoothing the vertical diffusivity profile with 4-, 5-, 6- and 8-point moving averages, and fitting simple spline curves. All linear interpolation schemes caused artificial aggregation of particles near sharp changes in diffusivity, even after data points were proliferated and then smoothed with a moving average. These results support the conclusions of Brickman and Smith (2001) who found that discontinuities in the vertical profile of K_v made demonstration of the WMC impossible. Although simple spline curves result in a smooth function, they caused artificial gaps in particle distributions because they added inflection points near sharp changes in vertical diffusivity.

The most reasonable results were obtained by fitting a tension spline to the water column profile of vertical diffusivity at the particle location. To do this, a five-step procedure was implemented:

1. Vertical diffusivities at sigma-levels at the x-y particle location were estimated with 4-point linear interpolation (Figure 2a), and sigma levels were transformed to positive and increasing z-coordinates (Figure 2b).
2. The number of data points between K_v grid points were proliferated with linear interpolation (Figure 2c).
3. An 8-point moving average was used to smooth the data. Surface and bottom boundary values were forced to equal minimum diffusivity in the hydrodynamic model.
4. A tension spline curve was fit to the data. (Figrue 2d).
5. The value of K_v' and K_v was calculated at the appropriate z-coordinate on the tension spline curve.

The tension spline curve was fit to the data using a subroutine and functions from the Tension Spline Curve Fitting Package (TSPACK). TSPACK (TOMS/716) was created by Robert J. Renka (renka@cs.unt.edu, Department of Computer Science, University of North Texas) and is available for download from www.netlib.org. Occasionally, the curve fitting method would fail to converge (~0.0004% of the time, or 1 time in 244,500 calls to TSPACK). In these rare cases, linear interpolation was used to estimate K_v and K_v' to avoid program pause. The curve fitting method in TSPACK was designed to "avoid extraneous inflection points (associated with rapidly varying data values) and preserve local shape properties of the data (monotonicity and convexity)." This is an important attribute of the tension spline that prevents addition of inflection points that occur when simple spline curves are implemented in the random displacement model.

Vertical boundary conditions. Reflective boundary conditions were specified for the surface and bottom boundaries (Brickman and Smith 2001, Proehl and Lynch 2001). If a particle passed through the surface or bottom boundary due to turbulence or vertical advection, the particle was placed back in the model domain at a distance from the boundary equal to the distance that the particle location exceeded the boundary.

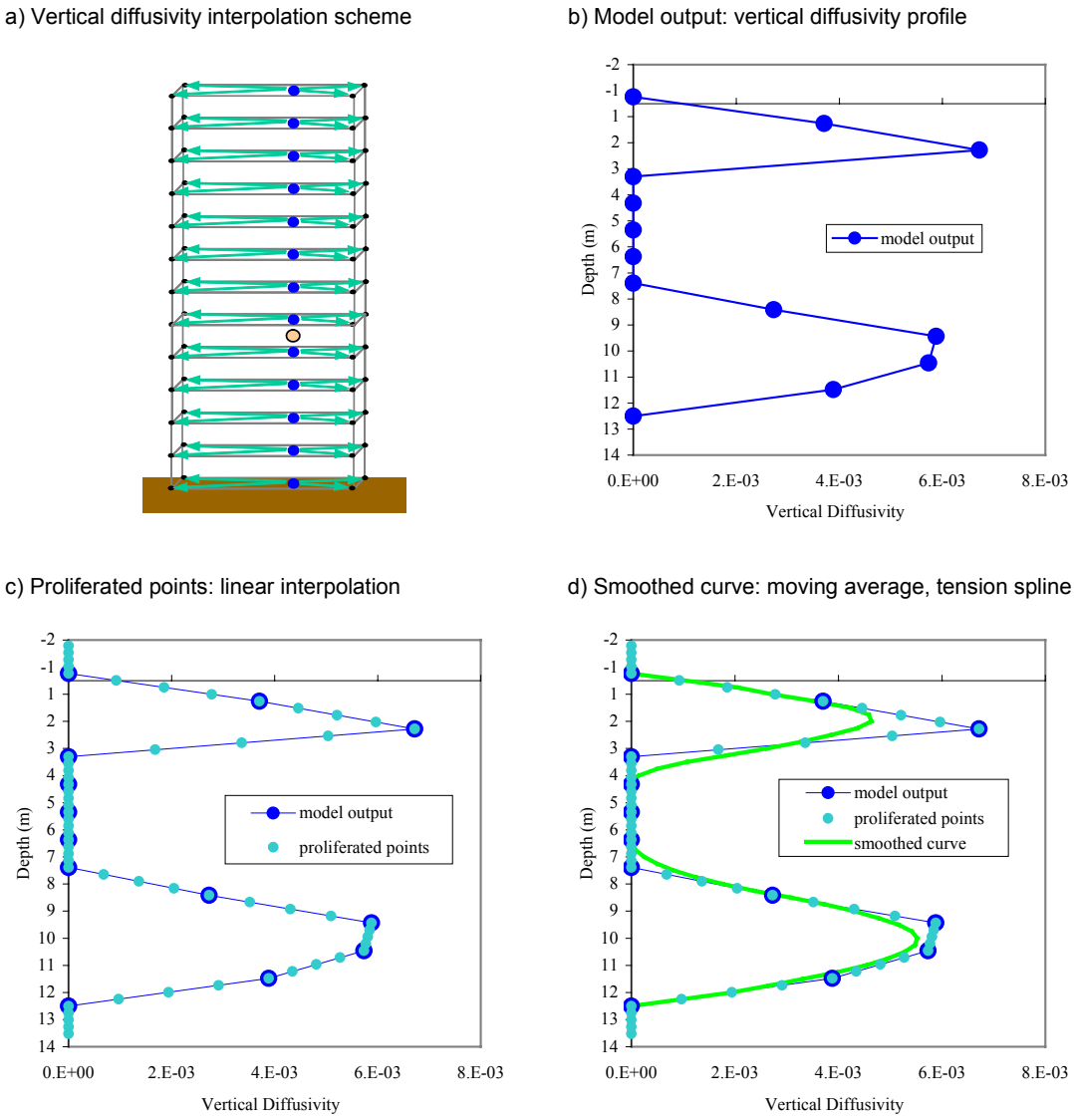

Figure 2. Procedure for implementing the random displacement model. a) Location of vertical diffusivity values (blue dots) at the x-y particle location (orange dot). Values were calculated with a 4-point linear interpolation scheme (green arrows). b) Vertical diffusivity profile output from the hydrodynamic model at river kilometer 35. c) Proliferated data points used to smooth data. d) The smoothed profile (8-pt moving average) of vertical diffusivity fit with a tension spline.

Horizontal boundary conditions. Advection is the dominant transport process in the hydrodynamic model. For tests of the Well Mixed Condition, particles needed to be retained within the bounds of the particle tracking model (6 to 90 river kilometers of the hydrodynamic model) and not advected downstream. To maintain particles within the particle tracking model boundary, particles were 'looped' between boundaries. If a particle hit the up-estuary boundary, it was placed at the down-estuary boundary at a randomly assigned depth, and vice versa.

Tests of the Well Mixed Condition. For tests of the Well Mixed Condition, 50,000 particles were released in an initially random distribution in a x-z plane in the center of the channel and tracked over 1 tidal cycle (12 hrs) during steady state conditions. After ~12 hrs, differential advection in the upper and lower water column (estuarine gravitational circulation) created differences in particle concentrations at the horizontal boundaries. These differences confounded WMC tests. In the WMC scenarios presented here, the number of particles per grid cell was ~50 (Proehl and Lynch 2001), a number that resulted in acceptable variance in the Lagrangian solution and allowed reasonable computation time.

A quantitative measure of the Well Mixed Condition was adapted from Brickman and Smith (2001). The 2D correlation test was based on the association (or lack of) between particle concentrations and vertical diffusivity in the model. If particles aggregated in regions of low diffusivity (e.g. Fig. 1c), then a negative correlation between particle concentrations and K_v was expected, indicating violation of the Well Mixed Condition. If there was no significant correlation between K_v and particle concentrations over time, then the Well Mixed Condition was demonstrated.

The procedure for the 2D correlation test had two steps: calculating correlation coefficients from model output and defining confidence intervals. To calculate correlation coefficients from model output, the number of particles in a box surrounding each K_v grid point was calculated, paired with the appropriate K_v value at the grid point, and correlation analyses were conducted. Although Brickman and Smith (2001) computed Pearson correlation coefficients, Spearman's rank-order correlation coefficients (r) were used to test for the WMC tests presented here (SAS v. 8.01) because K_v values from the hydrodynamic model were not normally distributed. Spearman correlation coefficients of model output were calculated every 0.25 hrs for each 12 hr model run. Five scenarios with a random displacement model were conducted with different initial conditions (i.e., 5 different initial random particle distributions). One scenario was conducted with a random walk model instead of a random displacement model.

Confidence intervals for correlation tests were defined as in Brickman and Smith (2001). Two thousand distributions of 50,000 particles were generated by placing particles randomly throughout the particle tracking model domain. Particle concentrations were calculated for each of the 2,000 random distributions, paired with K_v from the hydrodynamic model at a single time point, and Spearman correlation coefficients (r) were calculated. The minimum and maximum r values were selected to create 100% confidence intervals (Brickman and Smith (2001) used 95% confidence intervals). This procedure was repeated every 0.25 hrs for 12 hrs to determine the 100% confidence intervals over time. The correlation coefficients from the model output were compared to the confidence intervals. If outside the intervals, the model correlation coefficients were considered significantly different from those of randomly distributed particles and in violation of the WMC. If model correlation coefficients remained within the confidence intervals over time, then the WMC was considered satisfied.

Comparison of Lagrangian and Eulerian distributions. Model simulations were conducted to compare the distribution of an Eulerican tracer and Lagrangian particles when sub-grid scale turbulence was simulated with a random displacement model. At day 350, 5,000 neutrally buoyant particles and high concentrations of a neutrally buoyant Eulerian tracer were released at the same location in the hydrodynamic model. The model was run for 2 days and the concentrations of particles and tracer in each hydrodynamic grid cell were compared graphically and with Spearman correlation tests. Scenarios also were conducted with particles and tracer assigned the same constant sinking speed similar to small sediment particles (0.03 mm s^{-1}). In addition, neutrally buoyant and sinking tracer/particle scenarios were repeated with and without a wind event (approximately 9.1 m s^{-1} wind speed) that started on day 350.5 and ended on day 351.375 (21-hr).

RESULTS

Well Mixed Condition tests. When turbulent particle motion was parameterized with a simple random walk model in the vertical, model output did not pass the WMC correlation test (100% failure rate: all correlation coefficients were significantly different from random distributions). In contrast, 98.8% of correlation coefficients remained within the 100% confidence intervals during the 12 hr period when turbulent motion was parameterized with a random displacement model (a 1.2% failure rate).

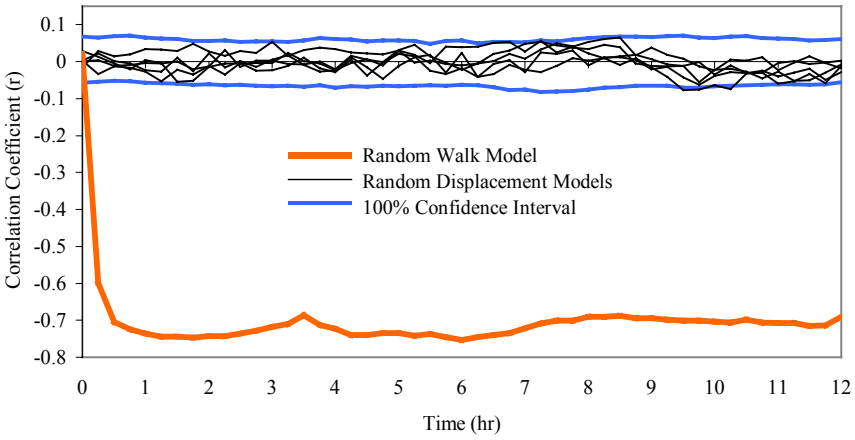

Fig. 3. Correlation coefficients (of particle concentrations versus vertical diffusivity) over time for two sub-grid scale turbulence models: Random Walk (thick orange line) and Random Displacement Models (thin black lines). Correlations coefficients that do not remain within the 100% confidence intervals (blue lines) violate the Well Mixed Condition, a necessary condition for simulating unbiased turbulent diffusion.

Results of the Well Mixed Condition tests were influenced by the time step of the particle tracking model itself. When the time step of the particle tracking model was equal to that of the hydrodynamic model (40 s), failure of the WMC increased. This was likely due to transient accumulations of particles near the surface and bottom boundaries within the region of the salt front convergence zone. As suggested by Proehl and Lynch (2001), increasing the temporal resolution of the particle tracking model appeared to alleviate this problem.

Another important consideration related to surface and bottom boundary conditions. According to Brickman and Smith (2001), theoretical work suggests that the gradient in vertical diffusivity should be zero at the boundaries of the model. We conducted model scenarios with the gradient in K_v forced to zero at the boundaries, but adding this parameterization did not improve particle tracking model performance.

Comparison of Lagrangian and Eulerian distributions. Figs. 4 and 5 summarize the results of the comparison between Eulerian tracer and Lagrangian particle distributions. Spearman correlation coefficients were positive and significant (α = 0.001) for all model output (Fig. 4), indicating that high particle concentrations coincided with high tracer concentrations. Comparison of correlation coefficients over time suggested that particles motion best approximated tracer dispersal when wind events increased mixing in the water column

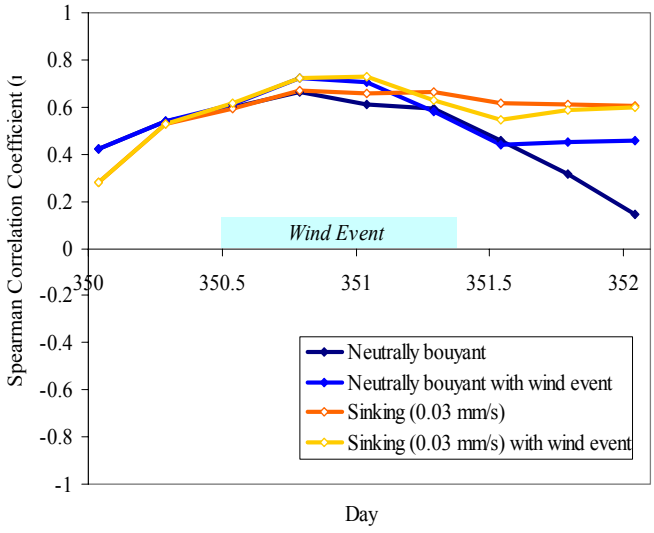

Fig. 4. Spearman correlation coefficients (r) over time of particle concentrations compared to Eulerian tracer concentrations.

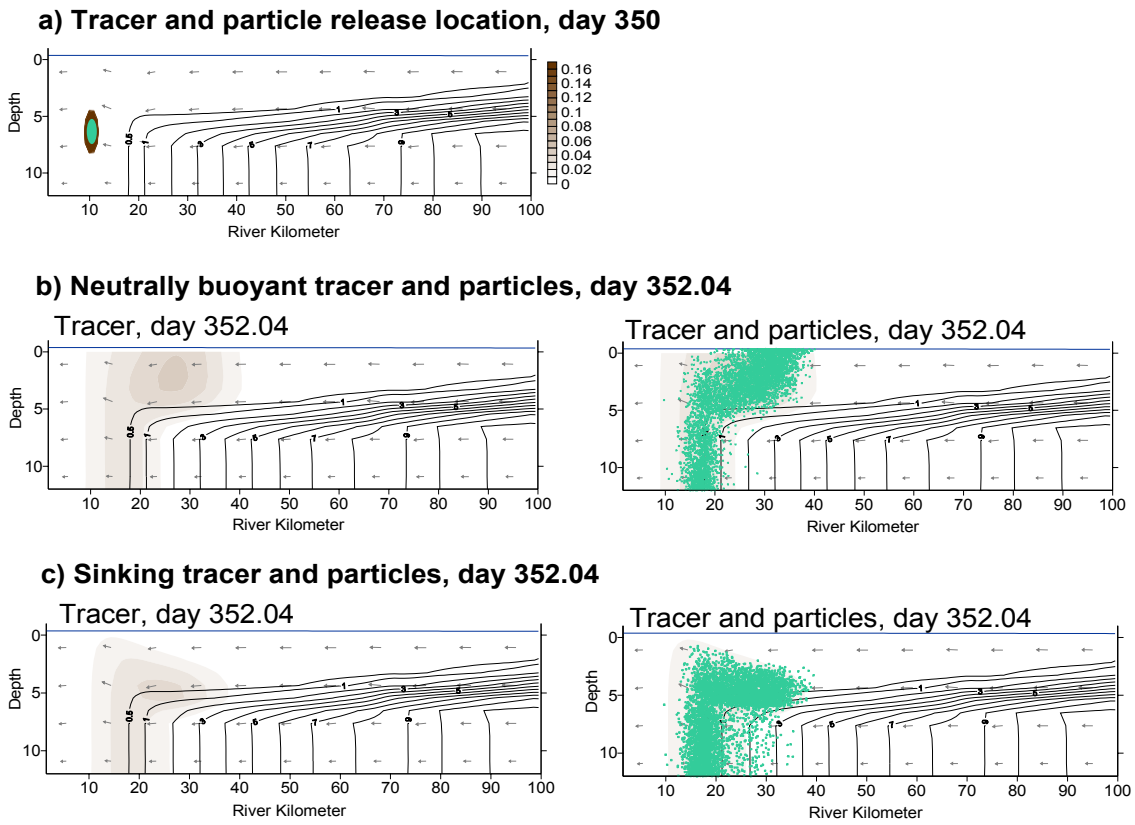

Fig. 5. Comparison of Eulerian tracer and Lagrangian particle distributions. a) Release location at day 350. b) Distribution of neutrally buoyant tracer and particles at day 352.04. b) Distribution of sinking tracer and particles at day 352.04 (sinking speed = 0.03 m s^{-1}).

or particles/tracers were assigned sinking speeds. Graphical comparison of particle and tracer distributions (Fig. 5) indicated relatively close agreement, although it was apparent that the Eulerian tracer spread horizontally at a faster rate than the particles. Agreement between Lagrangian and Eulerian solutions may be improved by increasing particle numbers and tuning the scaling coefficient (c) in the horizontal sub-grid scale turbulence model.

SUMMARY

A random displacement model was implemented within a Lagrangian particle tracking model that improved simulation of particle motion in a frontal region with sharp gradients in turbulence. Results of the Well Mixed Conditions test were encouraging and clearly supported the findings of Visser (1997) and Brickman and Smith (2001): the random displacement model is much preferred to a random walk model when simulating sub-grid scale turbulence in stratified conditions.

Comparison of the Eulerian tracer and Lagrangian particle distributions indicated reasonable agreement between the two models, although Eulerian tracer concentrations appeared to spread horizontally at a faster rate than Lagrangian particles. Results indicated that the coupled hydrographic-Lagrangian model successfully simulated turbulent particle motion in a frontal region, and suggest that this model has the potential to be a powerful tool for investigating the influence of hydrographic variability on the transport and survival of fish early-life stages in frontal zones.

ACKNOWLEDGEMENTS

Many thanks to Charles Hannah, Uffe Thygessen, and Tipani Stipa for their helpful advice and discussions. EN appreciates support from the National Science Foundation for attending the ICES Study Group on Modeling Physical-Biological Interactions meeting (March 200) during which some of these discussions occurred. This research was part of the Bio-physical Interactions in the Turbidity Maximum (BITMAX) program sponsored by the NSF Biological Oceanography Program award to SYC, RRH, LPS, E. D. Houde, M. R. Roman, and C. T. Friedrichs (Grant Number: OCE-0002543).

LITERATURE CITED

Allen, G.P., J. C. Salomon, P. Bassoullet, Y. Du Penhoat, and C. De Grandpré. 1980. Effects of tides on mixing and suspended sediment in macrotidal estuaries. Sediment Geology 26:69-80

Bartsch, J., and S. H. Coombs. 2001. An individual-based growth and transport model of the early life-history stages of mackerel (*Scomber scombrus*) in the eastern North Atlantic. Ecological Modeling 138:127-141.

Bennett, W. A., W. J. Kimmerer, and J. R. Burau. 2002. Plasticity in the vertical migration by native and exotic estuarine fishes in a dynamic low-salinity zone. Limnology and Oceanography 47(5):1496-1507.

Bergey, L. L., R. A. Rulifson, M. L. Gallagher, and A. S. Overton. *In press*. Variability of Atlantic coast striped bass egg characteristics. North American Journal of Fisheries Management

Bjorkstedt, E. P., L. K. Rosenfeld, B. A. Grantham, Y. Shkedy, and J. Roughgarden. 2002. Distributions of larval rockfishes *Sebastes* spp. Across nearshore fronts in a coastal upwelling region. Marine Ecology Progress Series. 242:215-228

Blumberg, A. F., and G. L. Mellor. 1987. A description of a three-dimensional coastal ocean circulation model. In: N. Heaps (ed.), Three-dimensional coastal ocean models, vol 4. American Geophysical Union, Washington, DC.

Boynton, W. R., W. Boicourt, S. Brant, J. Hagy, L. Harding, E. Houde, D.V. Holliday, M. Jech, W. M. Kemp, C. Lascara, S. D. Leach, A. P. Madden, M. Roman, L. Sanford, and E. M. Smith. 1997. Interactions between physics and biology in the estuarine turbidity maximum (ETM) of Chesapeake Bay, USA. International Council for the Exploration of the Sea CM 1997/S:11.

Brickman, D. and P. C. Smith. 2002. Lagrangian stochastic modeling in coastal oceanography. Journal of Atmospheric and Ocean Technology 19:83-99.

Burau, J. R., J. W. Gartner, and M. Stacey. 1998. Results from the hydrodynamic element of the 1994 entrapment zone study in Suisun Bay. In: W. Kimmerer (ed) Report of the 1994 Entrapment Zone Study. Interagency Ecological Program for the San Francisco Bay/Delta Estuary Technical Repot 56.

Dauvin, J.-C., and J. J. Dodson. 1990. Relationship between feeding incidence and vertical and longitudinal distribution of rainbow smelt larvae (*Osmerus mordax*) in a turbid well-mixed estuary. Marine Ecology Progress Series 60:1-12.

D'Anglejan, B. 1981. On the advection of turbidity in the Saint Lawrence middle estuary. Estuaries 4(10):2-15.

Dodson, J. J., J.-C. Dauvin, R. G. Ingram, and B. D'Anglejan. 1989. Abundance of larval rainbow smelt (*Osmerus mordax*) in relation to the maximum turbidity zone and associated macroplanktonic fauna of the middle St. Lawrence estuary. Estuaries 12(2):66-81.

Epifanio, C. 1987. The role of tidal fronts in maintaining patches of Brachyuran zoeae in estuarine waters. Journal of Crustacean Biology 7(3):513-517.

Epstein, A. W., R. C. Beardsley. 2001. Flow-induced aggregation of plankton at a front: a 2-D Eulerian model study. Deep-Sea Research (Part II, Topical Studies in Oceanography) 48(1-3):395-418.

Franks, P. J. S., and L. J. Walstad. 1997. Phytoplankton patches at fronts: a model of formation and response to wind events. Journal of Marine Research 55:1-29.

Geyer, W. R., J. D. Woodruff, and P. Traykovski. 2001. Sediment transport and trapping in the Hudson River estuary. *Estuaries* 24(5):670-679.

Govoni, J. J. 1993. Flux of larval fishes across frontal boundaries: Examples from the Mississippi River plume front and the western Gulf Stream front in winter. Bulletin of Marine Science 52(2):538-566.

Govoni, J. J. 1997. The association of the population recruitment of Gulf menhaden, Brevoortia patronus, with Mississippi River discharge. Journal of Marine Systems 12(1-4):101-108.

Govoni, J. J., and C. B. Grimes. 1992. The surface accumulation of larval fishes by hydrodynamic convergence within the Mississippi River plume front. Continental Shelf Research. 12(11):1265-1276.

Govoni, J. J., D. E. Hoss, and D. R. Colby. 1989. The spatial distribution of larval fishes about the Mississippi River plume. Limnology and Oceanography 34(1):178-187.

Hannah, C. G., C. E. Naimie, J. W. Loder, and F. E. Werner. 1998. Upper-ocean mechanisms from the Gulf of Maine to Georges Bank, with implications for *Calanus* supply. Continental Shelf Research 17(15):1887-1911.

Hare, J. A., J. A. Quinlan, F. E. Werner, B. O. Blanton, J. J. Govoni, R. B. Forward, L. R. Settle, and D. E. Hoss. 1999. Larval transport during winter in the SABRE study area: results of a coupled vertical behaviour-three-dimensional circulation model. Fisheries Oceanography 8(Supplement 2): 57-76.

Heath, M. R., and A. Gallego. 1998. Bio-physical modelling of the early life stages of haddock, *Melanogrammus aeglefinus*, in the North Sea. Fisheries Oceanography 7(2):110-125.

Hinckley, S. A. J. Hermann, K. L. Mier, and B. A. Megrey. 2001. Importance of spawning location and timing to successful transport to nursery areas: a simulation study of Gulf of Alaska walleye pollock. ICES Journal of Marine Science 58:1042-1052.

Hood, R. R., M. R. Abbott, A. Huyer. 1991. Phytoplankton and photosynthetic light response in the coastal transition zone off northern California in June 1987. Journal of Geophysical Research Oceans 96(C8): 14769-780.

Jassby, A. D., W. J. Kimmerer, S. G. Monismith, C. Armor, J. E. Cloern, T. M. Powell, J. R. Schubel, and T. J. Vendlinski. 1995. Isohaline position as a habitat indicator for estuarine populations. Ecological Applications 5(1):272-289.

Jay, D. A., and J. D. Musiak. 1994. Particle trapping in estuarine tidal flows. Journal of Geophysical Research 99(C10):20,445-20,461.

Jillett, J. B., and J. R. Zeldis. 1985. Aerial observations of surface patchiness of a planktonic crustacean. Bulletin of Marine Science 37 (2):609-619

Kappenberg, J., and I. Grabemann. 2001. Variability of the mixing zones and estuarine turbidity maxima in the Elbe and Weser estuaries. Estuaries 24(5):699-706.

Kingsford, M. J., and I. M. Suthers. 1996. The influence of tidal phase on patterns of ichthyoplankton abundance in the vicinity of an estuarine front, Botany Bay, Australia. Estuarine, Coastal and Shelf Science 43(1):33-54.

Kostaschuk, R. 2002. Flow and sediment dynamics in migrating salinity intrusions: Fraser River estuary, Canada. Estuaries 25(2):197-203

Largier, J. L. 1993. Estuarine fronts: how important are they? Estuaries 16(1): 1-11.

Lin, J., and A. Y. Kuo. 2001. Secondary turbidity maximum in a partially mixed microtidal estuary. Estuaries

24(5):707-720.

Lough, R. G., and J. P. Manning. 2001. Tidal-front entrainment and retention of fish larvae on the southern flank of Georges Bank. Deep Sea Research II 48: 631-644.,

Mackas, D. L. and G. C. Louttit. 1988. Aggregation of the copepod *Neocalanus plumchrus* at the margin of the Fraser River plume in the Strait of Georgia. Bulletin of Marine Science 43(3): 810-824.

Mellor, G. L. 1998. User's guide for a three-dimensional, primitive equation, numerical ocean model. Program in Atmospheric and Ocean Sciences, Princeton University, New Jersey. 44 pp.

Mellor, G. L. and T. Yamada. 1974. A hierarchy of turbulence closure models for planetary boundary layers. Journal of Atmospheric Science 31:1791-1806.

Munk, P., P. O. Larsson, D. S. Danielssen, and E. Moksness. 1999. Variability in frontal zone formation and distribution of gadoid fish larvae at the shelf break in the northeastern North Sea. Marine Ecology Progress Series 177: 221-233.

Munk, P., P. J. Wright, N. J. Pihl. 2002. Distribution of the Early Larval Stages of Cod, Plaice and Lesser Sandeel across Haline Fronts in the North Sea. Estuarine, Coastal and Shelf Science 55(1): 139-149.

Nakata, H., S. Kimura, Y. Okazaki, and A. Kasai. 2000. Implications of mesoscale eddies caused by frontal disturbances of the Kuroshio Current for anchovy recruitment. ICES Journal of Marine Science 57(1): 143-152.

North, E. W., S.-Y. Chao, L. P. Sanford, and R. R. Hood. *In press*. The influence of wind and river pulses on an estuarine turbidity maximum: numerical studies and field observations in Chesapeake Bay. Estuaries.

North, E. W., and E. D. Houde. 2001. Retention of white perch and striped bass larvae: biological-physical interactions in Chesapeake Bay estuarine turbidity maximum. Estuaries 24(5): 756-769.

North, E. W., and E. D. Houde. *In press*. Linking ETM physics, zooplankton prey, and fish early-life histories to white perch (*Morone americana*) and striped bass (*M. saxatilis*) recruitment success. Marine Ecology Progress Series.

Okazaki, Y., H. Nakata, Y. Iwatsuki. 1998. Distribution and food availability of fish larvae in the vicinity of a thermohaline front at the entrance of Ise Bay Fisheries science. 64(2): 228-234.

Proehl, J. A. and D. R. Lynch. 2001. Experiments in Lagrangian diffusion. Numerical Methods Laboratory Report #NML-01-5, Dartmouth College. December 1, 2001.

Raudkivi, A. J. 1990. Loose boundary Hydraulics, 3rd edition. Pergamon Press, Oxford

Sanford, L.P., S. E. Suttles, and J. P. Halka. 2001. Reconsidering the physics of the Chesapeake Bay estuarine turbidity maximum. Estuaries 24(5):655-669.

Schubel, J. R. 1968. Turbidity maximum of the northern Chesapeake Bay. Science 161:1013-1015.

Shanks, A. L., J. Largier, L. Brink, J. Brubaker, and R. Hooff. 2000. Demonstration of the onshore transport of larval invertebrates by the shoreward movement of an upwelling front. Limnology and Oceanography 45(1): 230-236.

Sirois. P., and J. J. Dodson. 2000. Influence of turbidity, food density and parasites on the ingestion and growth of larval rainbow smelt *Osmerus mordax* in an estuarine turbidity maximum. Marine Ecology Progress Series 193:167-179.

Uncles, R. J., and J. A. Stephens. 1993. The freshwater-saltwater interface and its relationship to the turbidity maximum in the Tamar estuary, United Kingdom. Estuaries 16(1):126-141.

Uye, S.-I., T. Yamaoka, and T. Fujisawa. 1992. Are tidal fronts good recruitment areas for herbivorous copepods? Fisheries Oceanography 1(3): 216-226

Visser, A. W. 1997. Using random walk models to simulate the vertical distribution of particles in a turbulent

water column. Marine Ecology Progress Series 158: 275-281.

Werner, F. E., R. I. Perry, R. G. Lough, and C. E. Naimie. 1996. Trophodynamic and advective influences on Georges Bank larval cod and haddock. Deep-Sea Research II 43(7-8): 1793-1822.

Werner, F. E., B. R. MacKenzie, R. I. Perry, R. G. Lough, C. E. Naimie, B. O. Blanton, and J. A. Quinlan. 2001. Larval trophodynamics, turbulence, and drift on Georges Bank: a sensitivity analysis of cod and haddock. Scientia Marina 65(Supplement 1):99-115.

Winkler, G., J. J. Dodson, N. Bertrand, D. Thivierge, W. F. Vincent. 2003. Trophic coupling across the St. Lawrence River estuarine transition zone. Marine Ecology Progress Series 251: 59-73

Wolanski, E., and W. M. Hamner. 1988. Topographically controlled fronts in the ocean and their biological influence. Science 241:177-181.